# Natural polysaccharides and microfluidics: A win–win combination towards the green and continuous production of long-term stable silver nanoparticles

Antonella Giorello[a], Esteban Gioria[a], Jose L. Hueso[b,c], Victor Sebastian[b,c], Manuel Arruebo[b,c], Carolina Veaute[d], Laura Gutierrez[a,*]

[a] *Instituto de Investigaciones en Catálisis y Petroquímica, INCAPE, (FIQ, UNL-CONICET), Santiago del Estero 2829, S3000, Santa Fe, Argentina*

[b] *Institute of Nanoscience of Aragon (INA), Department of Chemical and Environmental Engineering, Edificio I+D+i, Campus Rio Ebro, 50018, Zaragoza, Spain* [c] *Networking Research Center on Bioengineering, Biomaterials and Nanomedicine (CIBER-BBN), 28029, Madrid, Spain*

[d] *Laboratorio de Inmunología Básica, FBCB, Universidad Nacional del Litoral, UNL, Ciudad Universitaria UNL, Ruta Nacional Nº 168, Km 472, S3000ZAA, Santa Fe, Argentina*

ABSTRACT

**The present work combines the use of microfluidic reactors and green chemicals such as glucose and starch to achieve a continuous production of silver nanoparticles that have been successfully tested as excellent antibacterial agents against *Escherichia coli*. Those silver nanoparticles synthesized under continuous flow remained stable in terms of optical response, morphology and size distribution even after 48 months of storage at 24 °C without light protection. The best results in terms of colloidal stability were obtained after synthesizing those** nanoparticles **at 70 °C in the presence of an excess of glucose when the continuous flow configuration was used to complete the reaction within 9 min. In contrast, analogous experiments carried out in batch conditions re- quired a much longer period to achieve similar results but with much lower stability and a higher polydispersity, especially in the long-term storage range.**

## 1. Introduction

Metal nanoparticles (i.e., mainly Au, Cu and Ag), have been extensively evaluated as antimicrobial agents. Infections caused by bacteria demand prolonged and not always successful treatments that affect negatively mortality and morbidity rates [1,2]. In particular, the bactericidal activity of silver nanoparticles (Ag NPs) has been attributed to the combined action of several mechanisms such as the production of reactive oxygen species (ROS), induced gene modification, cell-wall penetration and damage, and protein and DNA interactions [3–6]. Great efforts are being devoted to synthesize Ag NPs as silver-ion reservoirs in paints, textile fibers and surgery materials in order to generate aseptic surfaces [7,8]. In addition, Ag NPs uses are extended to many others applications such as water treatment, coatings on catheters, prosthesis, on surfaces used in the food industry, food packaging, etc [9].

The wet chemical reduction of silver precursors in batch systems is the most widespread method for Ag NPs synthesis. The use of hazardous reducing agents, such as sodium borohydride ($NaBH_4$) or hydrazine ($N_2H_4$) is much extended. Furthermore, there is a strong motivation in applying the Green Chemistry concepts to in the material synthesis routes [10].

Consequently, different biological molecules have been evaluated as reducer agents for Ag NPs synthesis following safe, sustainable and eco-friendly procedures. For instance, microorganisms (bacteria, fungi actinomycetes, yeast and viruses,) acting as bioreactors have been reported to produce a variety of nanoparticles either intra or extra-cellularly [11]. Plant extracts from stems, flowers, leaves and seeds have also been studied as green reducers and stabilizers materials for NPs synthesis [12]. Although both synthesis employing either microorganisms or vegetable extracts are in agreement with the main green principles, the use of the former implies highly strict pH and temperature working ranges or lack of sufficient control on the chemical composition of the latter.

Polysaccharides have also been proposed as green reducer agents as they are able to replace the need for toxic solvents and they can also act as easy particle separation agent [13]. In the literature, there are a great number of examples where glucose and starch have been tested either as reducing agents [14–16], or as capping ligands [16,17]. Likewise, the combination of glucose acting as reductant and starch as co-stabilizer has been also evaluated [18–21].

Glucose and starch have high market availability with stable

formulation and low cost. In contrast, natural plant extracts that exhibit an analogous and promising role as effective reductors for the generation of NPs, require tedious, time-consuming purification steps that so far are preventing their commercialization.

The use of microfluidic systems for processing liquid phases to render nano-scaled materials has been taken into account as green process. Continuous material synthesis technology leads to a larger number of advantages compared with the batch-to-batch approach. Sebastian et al. [22] pointed out, "Microreactors constitute perhaps the enabling technology of the highest potential for liquid phase synthesis of Engineered nanomaterials (ENMs)" [23,24].

An intensive search of the reported works during the last ten years reveals the increasing efforts to find better alternatives for the Ag NPs production (Table S1). Although several authors studied glucose as reducing agent, the number of studies evaluating the use of glucose in a continuous synthesis is still scarce [18,19,21,25–29]. Horikoshi et al. [29] evaluated the Ag NPs synthesis employing glucose and microreactors and obtained narrow size distributions compared with the materials retrieved from conventional batch methods. Nevertheless, their studies did not validate the stability of the resulting Ag NPs suspensions for extended aging periods beyond 2–3 months [18,25,28].

Herein, we have combined the use of green chemicals such as glucose and starch and microfluidic reactors to achieve a continuous production of Ag NPs. The reaction condition effects on the Ag NPs optical response, morphology and size distribution were studied. The characteristics of the obtained suspensions were monitored in some cases for up to 48 months in order to evaluate their colloidal stability. A systematic comparison between the batch and continuous systems was performed. The Ag NPs synthesized were additionally tested as antibacterial agents against *Escherichia coli*. Therefore, a bacterial model (*E. coli*) irrespectively of its nature have just used in order to demonstrate the antimicrobial action of those materials. Actually, it is more difficult to treat gram-negative bacteria in comparison to gram-positive bacteria due to the presence of a membrane around the cell wall of gram-negative bacteria, which increases the risk of toxicity to the host being this membrane absent in gram-positive bacteria. In addition, porin channels are present in gram-negative bacteria, which can prevent the entry of drugs and antibiotics. These channels can also expel out antibiotics making much more difficult to treat in comparison to gram-positive bacteria. Finally, gram-negative bacteria possess both exotoxins and endotoxins but in case of gram-positive bacteria only exotoxins are produced [1]. Therefore, we chose *E. coli* due to the challenge that it represents and it was possible to corroborate that the glucose and starch do not inhibit the bactericidal effect of the synthesized nanoparticulated material.

## 2. Material and methods

### 2.1. Materials

For the Ag NPs synthesis, $AgNO_3$ (99.99%, Sigma-Aldrich) was used as metal precursor, β-D-Glucose (Cicarelli) as reductant and starch (Anedra) as stabilizing agent. All chemicals were pure (analytical grade) and used without further purification. Deionized water (18mΩ.cm) was used for the preparation of solutions in all the experiments. The nutrient culture media, Luria-Bertani (LB) broth, used in the antibacterial assays was prepared with meat peptone (Britania), yeast extract (Britania) and sodium chloride (Cicarelli). *E. coli* DH5-α strain was used as a model of Gram-negative microorganism.

### 2.2. Synthesis of silver nanoparticles

A modified protocol of a previous work described elsewhere was optimized to carry out the batch synthesis of silver nanoparticles in the presence of D(+)-glucose and starch used as reducer and capping agents, respectively [18]. The batch synthesis was carried out mixing a solution of $AgNO_3$ (0.01 M) with a solution of starch (0.17 wt. %) and glucose to achieve silver to glucose ratios (r = Ag/glucose) of 5/1; 1/1 and 1/5. The reaction time was fixed 6 h in contrast to 20 h as the reference protocol. The system was magnetically stirred in a round flask immersed in a thermostatic glycerin bath under refluxing conditions at 40, 55 and 70 °C (Table 1). For the continuous synthesis (Fig. 1), two syringe pumps (KD Scientific, KDS1000 model) fed the interdigital stainless steel-based microreactor provided by the Microelectronics Institute of Mainz (Germany) (Fig. 1c and d). At the outlet, a transparent Tygon® tubing (1.3 mm i.d.) was used to set a residence time of 9 min. Two stock solutions, one containing the $AgNO_3$ aqueous solution and the other containing the reducer-stabilizer aqueous mixture (glucose-starch) were loaded into two separated syringes and pumped into the micromixer with 8.8 mL/h as total flow rate. The micromixer and the aging tubing were immersed in a thermostatic glycerin bath in order to control the reaction temperature. The reaction time on both systems (batch and continuous) was established by macroscopic observations, when the yellowish color attributable to the formation of Ag NPs appeared. Furthermore, these parameters were set at reaction temperatures of 40 °C and 1/1 reactant ratios; those conditions were kept identical for the remaining syntheses and reaction conditions.

Table 1
Summary of the different synthesis conditions explored and the corresponding nomenclature assignation for each resulting Ag NPs suspension according to those parameters.

| Ratio Concentration ([Ag]/[glucose]) | Reaction Temperature (°C) | | | | | |
|---|---|---|---|---|---|---|
| | T = 40 | | T = 55 | | T = 70 | |
| | B | C | B | C | B | C |
| 1 stands for 5/1 ratio | B40_1 | C40_1 | B55_1 | C55_1 | B70_1 | C70_1 |
| 2 stands for 1/1 ratio | B40_2 | C40_2 | B55_2 | C55_2 | B70_2 | C70_2 |
| 3 stands for 1/5 ratio | B40_3 | C40_3 | B55_3 | C55_3 | B70_3 | C70_3 |

B: Batch system, residence time: 6 h; C: Continuous system, residence time: 9 min. All the experiments were duplicated and labeled as "a" or "b" at the end of the naming code.

Table 1 summarizes all the reaction conditions explored and the corresponding nomenclature assigned to each Ag NPs sample according to those synthesis parameters. Different reaction temperatures (40 °C, 55 °C and 70 °C) and Ag to glucose molar ratios (r = 5/1, 1/1 and 1/5) were selected to evaluate the effect of the reaction conditions on the Ag NPs morphology and stability. Finally, the suspensions were kept under ambient conditions for up to 48 months to evaluate long-term aging effects. They were stored in Eppendorf like tubes without any specific precaution (i.e. light protection) and were systematically evaluated at different time points.

### 2.3. Characterization techniques

UV–vis spectroscopy measurements were carried out in a double-beam UV–vis spectrophotometer PerkinElmer Lambda 40 without any sample washing treatment or dilution. The shape and average size of the nanoparticles were analyzed by Transmission Electron Microscopy (TEM) using a FEI Tecnai T20 microscope operating at 200 kV. The size distribution of the resulting colloidal nanoparticles was determined from the enlarged micrographs, using ImageJ free software [30] counting at least 200 particles. Size distribution was assessed using boxplot with R free software [31].

In order to study the reproducibility and the influence of the synthesis parameters (temperature and reagent ratios), samples of Ag NPs were prepared by duplicate and the Surface Plasmon Resonance (SPR) was determined just after synthesis ($t_0$). The stability studies for each synthesis conditions were monitored by UV–vis measurements of the absorbance and the evolution of the SPR response after 8 ($t_1$), 32

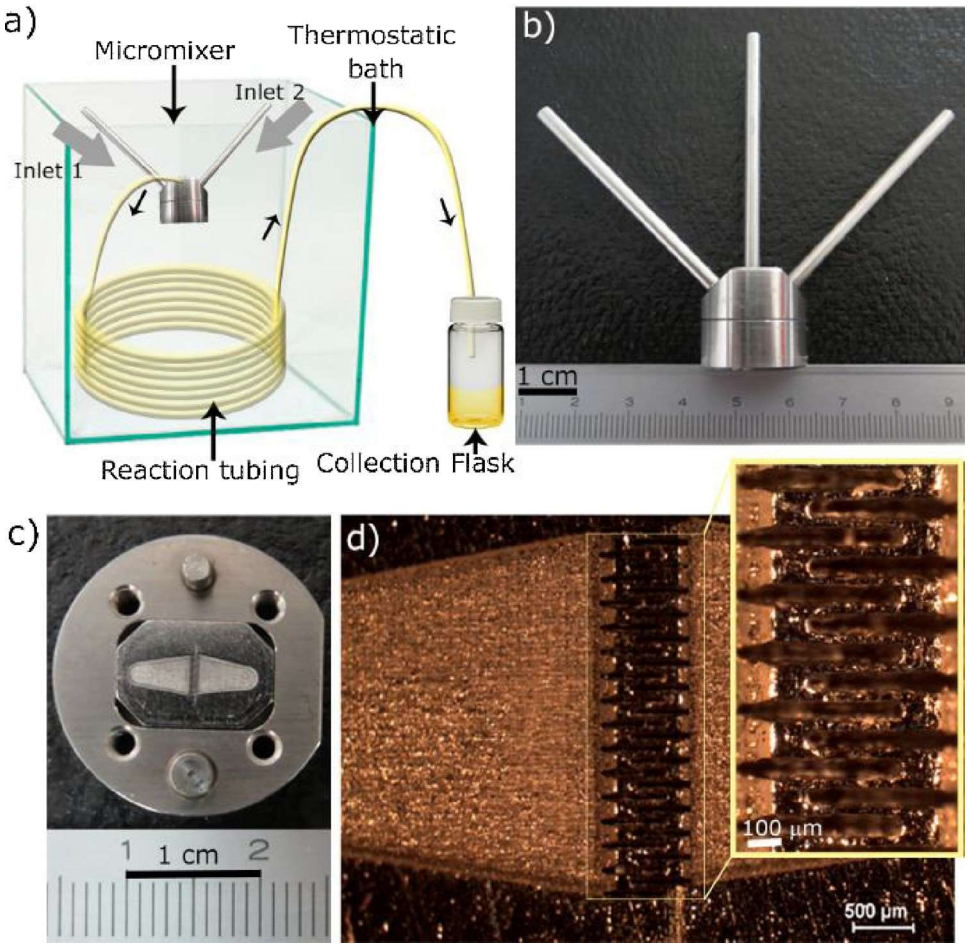


Fig. 1. a) Scheme of the experimental configuration displayed for the continuous synthesis of nanoparticles; b) Digital photograph of the standard slit interdigital microstructured mixer; c) Digital photograph of the interdigital device bottom plate; d) Optical image detailing the interdigital microchannels.

($t_2$) and 48 ($t_3$) months, respectively.

### 2.4. Bactericidal assays

After the characterization of the synthesized nanoparticles, the most stable set of suspensions was selected to evaluate the bactericidal activity using the viable cell colony count method. A single colony of *E. coli* was cultured in LB broth in an orbital shaker at 37 °C for 24 h, to reach stationary phase (ca.$10^9$ CFU/mL). For the experiment, 1 ml of *E.coli* (ca.$2.5 \times 10^6$ CFU/mL) was mixed with 1 ml of Ag NPs or $AgNO_3$ at two different concentrations (to achieve final concentrations (9 and 27 ppm) of Ag based on the original amount of silver nitrate used to prepare the NPs). The samples were incubated at 37 °C at 180 rpm. After 20 h, the samples were taken out, serially diluted with PBS and plated on LB agar plates. The plates were incubated at 37 °C for 24 h, and the viability was calculated by counting bacterial colonies on the plate. Control experiments were performed under identical conditions including a positive control in the absence of Ag NPs and a negative control in the absence of bacteria. Each experiment was carried out by triplicate. Data were compared using one-way ANOVA and Tukey-Kramer´s post hoc test, in GraphPad Prism 5. Results are expressed as means ± SD of measurements and different letters indicate significant differences between groups ($p < 0.05$).

## 3. Results and discussion

### 3.1. Influence of temperature and reactant ratios on the silver nanoparticles synthesis

Fig. 2 shows the UV–vis spectra of the suspensions prepared by duplicate (and labeled as “a” or “b” in the standard nomenclature described in Table 1) taken at the synthesis day ($t_0$) following batch (B) and continuous (C) methods at different reaction temperatures and Ag/glucose molar ratios (r).

The SPR maximum (Fig. 2) centered at ca. 420 nm and the spectra profiles were reproducible for both replicas and all the synthesis conditions. Fig. 2 shows that temperature, together with the reaction device set up, became a relevant factor influencing the outcome of the optical response. The experiments carried out at the lower temperatures (i.e. 40 °C and 55 °C) barely exhibited the presence of the SPR band at ca. 420 nm (Fig. 2a–d, g–j and m–o) or displayed a very broad absorption band suggesting the presence of polydispersed Ag NPs (Figs. 3a,b and S1). This latter effect was especially significant under batch conditions (Fig. 2 and Table 2). In contrast, higher temperatures led to a more effective silver reduction step to induce a major number of nucleation events, supported by sharper and more intense SPR bands with narrower full-width at half-maximum.

TEM images were also acquired to evaluate size distributions of the freshly prepared Ag NPs ($t_0$). A selection of representative TEM images has been displayed in Figs. 3 and S1. The particle size distribution was not very homogeneous in the batch reactor at 40, 55 or 70 °C and regardless of the precursor ratios (see Table 2 and Figs. S1–S2). In

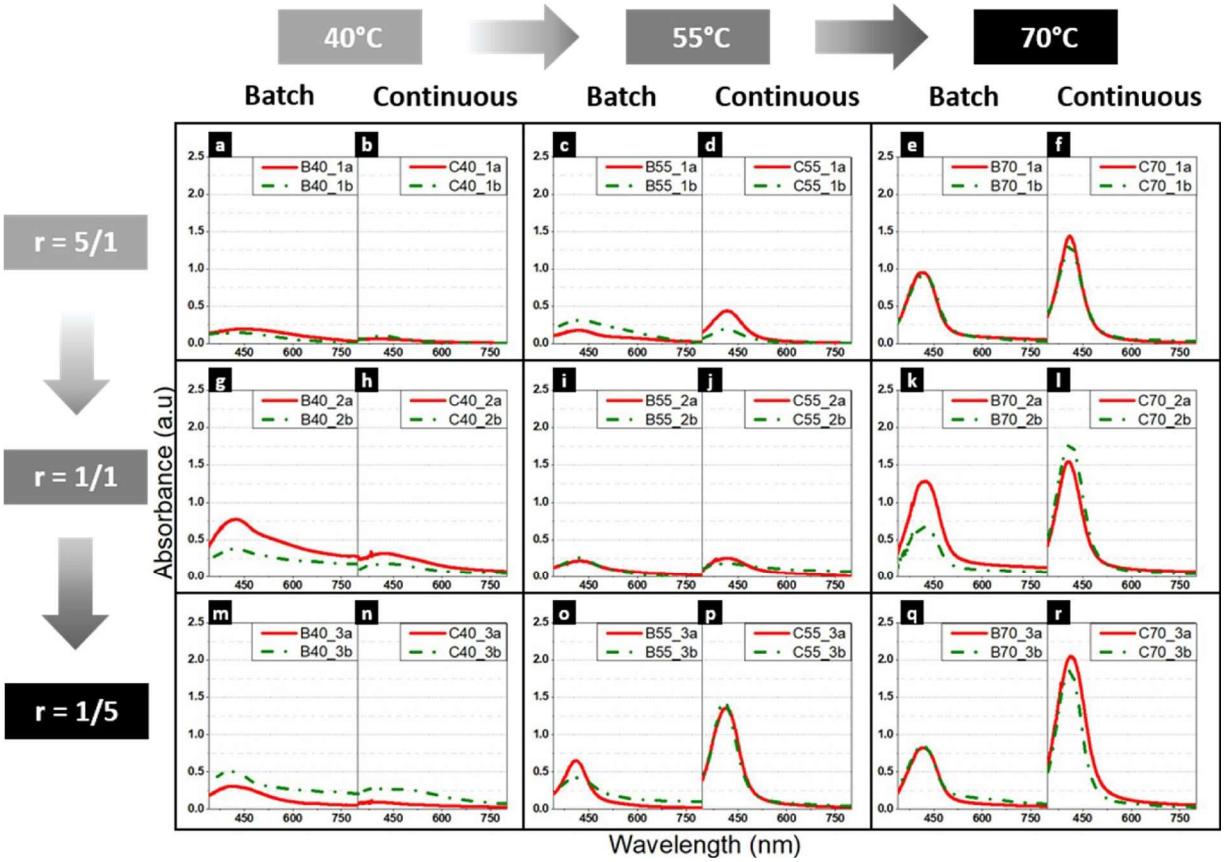


Fig. 2. Reproducibility study. UV–vis spectrum of the Ag NPs synthesis with discontinuous and continuous methods by duplicated replicas (a and b) at synthesis day ($t_0$). Reaction conditions: see also Table 1.

contrast, the continuous microfluidic setup led to more monodispersed size distributions when the reaction was carried out at 55 and 70 °C for all r-values (see Table 2, Figs. 3d–f and S1–S2).

These results are in agreement with previous findings reported in the literature. For instance, Jiang et al. [32] observed that low temperatures (ca. 0 °C) could significantly inhibit both particle formation and growth processes. In contrast, these authors observed that in the temperature range from 17 to 55 °C the reaction rate and the particle sizes increased. In this regard, Bonatto et al. [33] also found an important influence of the reaction temperature (75 °C) over the reducing effect on the synthesis of Ag NPs. In contrast, Vigneshwaran et al. [17] pointed out that at 120 °C the reduction reaction is accelerated by the presence of aldehyde functional groups, which are present in the carbohydrates molecules.

Remarkably, the temperature effect in the Ag NPs synthesis became more evident when the continuous microfluidic system was used. In fact, when the synthesis temperature reached 70 °C the UV–vis spectra rendered sharper and narrower SPR bands (Fig. 2f, l and r) than those obtained at 55 °C (Fig. 2d, j and p) and 40 °C (Fig. 2b, h and n), respectively. This result is attributable to the reaction conditions inherent to the use of the micromixer that favors a more homogeneous temperature distribution and a more efficient mixing of the reactants in the mixing process (Figs. 3f and S2). Previous works corroborated that microreactors enhance the monodispersity of the resulting nanoparticles while reducing the consumption of reactants [24,34].

The influence of glucose as reducing agent was also evaluated systematically varying the Ag/glucose molar ratios (r) in the synthesis process (Table 1 and Fig. 2). Taking into account the stoichiometry of the reduction reaction (r = 2/1) involving the silver nitrate precursor and glucose [35], the first selected ratio was glucose-deficient (r = 5/1) while the other ratios were carried out with an equimolar or an excess of glucose (r = 1/1 and 1/5).

In this context, it was expected that at initial reaction times, the higher the glucose concentration, the more favorable the reduction of silver would be and, consequently, the higher the SPR band intensity. In batch conditions, there is a slight trend showing an increase on the SPR intensity when the reaction occurs under excess of glucose (Fig. 2o). El-Rafie et al. [16] evaluated maize starch as reducer and stabilizer to generate Ag NPs in alkaline conditions. These authors compared the redox potential of glucose and starch under similar reaction temperature ranges (50–80 °C) and they identified a strong reducing capacity of glucose compared with that attributed to starch and fructose. Even though the starch is a non-reducing carbohydrate, those authors showed that alkaline conditions promoted the decomposition of the starch polymeric chains into fragments with reducing effects. Furthermore, rising the temperature to 60 and 80 °C also increased the redox potential of starch. Consequently, the temperature could play an important role on the acceleration of the reduction reaction and on the production of more reducing fragments coming from the starch.

On the other hand, they also concluded that the use of strong reductants led to smaller and less polydispersed nanoparticles while milder reducing conditions resulted in lower reduction rates. In this regard, Batabyal et al. [35] observed that an aqueous solution of $AgNO_3$ was not reduced by starch at room temperature. It is generally well established that a hydrothermal treatment of starch leads to glucose formation as the mayor hydrolysis product [35]. These findings are in agreement with our observations. In order to corroborate this effect, the synthesis of Ag NPs at 70 °C and r = 1/5 was performed in absence of starch, the UV–vis response resulted in a spectrum intensity lower than the corresponding to the synthesis containing the stabilizer (Fig. S3). This result suggests the reducing effect of the starch. On the other hand, this suspension after 20 days of storage presented a precipitate having

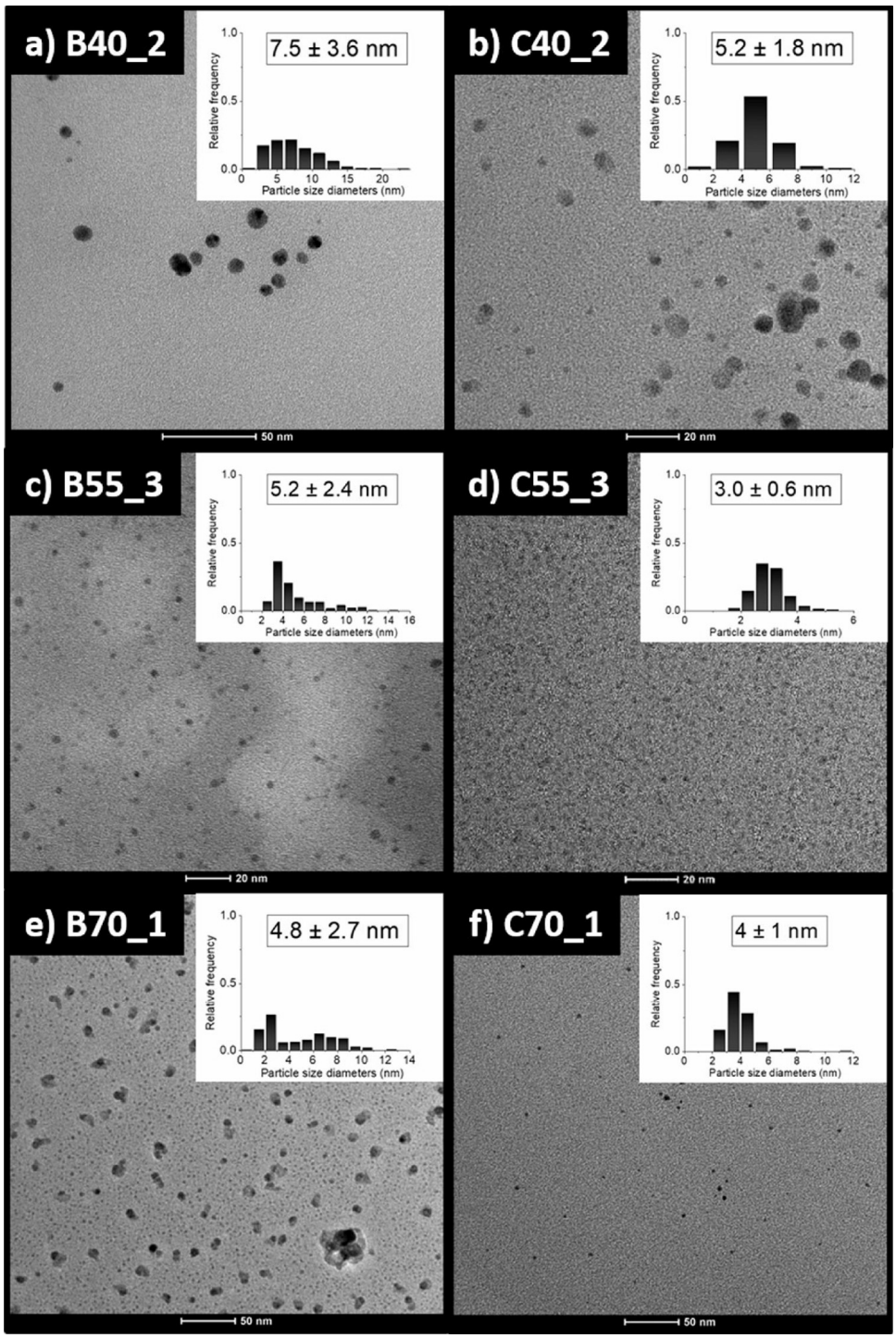


Fig. 3. Representative TEM images and corresponding particle size distributions of Ag NPs displaying the most promising plasmonic response and prepared at 40, 55 and 70 °C (initial $t_0$). Same information for other samples are shown in Fig. S1.

Table 2
Particle size distribution determined from TEM images at initial times ($t_0$) and after 48 months $t_3$ (sizes in nanometers).

| | | B | C | | | B | C | | | B | C |
|---|---|---|---|---|---|---|---|---|---|---|---|
| 40_1 | $t_0$ | 5.5 ± 2.5 | 2.6 ± 0.8 | 55_1 | $t_0$ | 12 ± 10 | 3.8 ± 1.2 | 70_1 | $t_0$ | 4.8 ± 2.7 | 4 ± 1 |
| | $t_3$ | 5.9 ± 10.3 | na | | $t_3$ | na | 48.3 ± 73.1 | | $t_3$ | 2.0 ± 1.9 | 6.3 ± 9.2 |
| 40_2 | $t_0$ | 7.5 ± 3.6 | 5.2 ± 1.8 | 55_2 | $t_0$ | 11.3 ± 10.6 | na | 70_2 | $t_0$ | 14 ± 15 | na |
| | $t_3$ | na | 5.7 ± 1.9 | | $t_3$ | na | 4.2 ± 1.4 | | $t_3$ | 14.3 ± 15.3 | 5.1 ± 6.9 |
| 40_3 | $t_0$ | na | 1.9 ± 0.7 | 55_3 | $t_0$ | 5.2 ± 2.4 | na | 70_3 | $t_0$ | 10.2 ± 10.8 | 1.7 ± 1.7 |
| | $t_3$ | 3.7 ± 1.8 | na | | $t_3$ | na | na | | $t_3$ | 14.0 ± 21.8 | 4.3 ± 5.4 |

na: No available.

large particles and its corresponding UV–vis plasmon disappeared completely, appearing the signal assigned to ionic silver at 288 nm. Therefore, these results confirm the role of starch as stabilizer and reducing agent. It is also worth mentioning that the intensity of the SPR signal was also much stronger in the presence of starch than in its absence (Fig. S3).

Finally, the experiments performed with lower concentration of glucose showed that the reduction mainly took place at the highest reaction temperatures (Fig. 2e and f), thereby reinforcing the potential role of starch as co-reducing agent. Interestingly, this effect seems to be even more effective with the continuous flow configuration in the microreactor. In contrast to the batch configuration, the microreactor induced a more intimate and homogeneous mixture of the reactants [24,34,36], especially at 70 °C (Figs. 2f, l, r, 3f and S2). A more efficient precursor mixture can lead to an enhanced grafting of the organic stabilizer on the surface of the growing crystals and to a consequent better control on the diffusion of the nutrients into the growing crystals, rendering homogeneous particles and subsequent narrow SPR peaks.

### 3.2. *Evaluation of the stability of silver nanoparticles after long-term storage periods*

UV-vis spectroscopy was used as a simple and reliable method for monitoring the stability of the nanoparticle suspensions at different time intervals. Fig. 4 shows the evolution of the SPR band for the different Ag NPs suspensions prepared with the batch and the continuous set up, respectively. Spectra acquisition took place after storing the samples under ambient conditions for 8, 32 and 48 months, ($t_1$, $t_2$ and $t_3$, respectively). In the case of batch synthesis, the SPR intensity increased with increasing aging times, especially after 32 months, suggesting that the reduction reaction was not concluded within the established reaction time or that larger NPs formed could have been dissolved progressively over time to generate smaller NPs.

The aged Ag NPs followed a similar trend in the continuous process and the intensity of the SPR band was higher at $t_1$ and $t_2$ than the observed at $t_0$. However, in this case, the differences established between the SPR intensity at initial times $t_0$ and $t_2$ were much less relevant in comparison with the batch experiments, especially at higher temperatures and in the presence of higher concentrations of glucose (Fig. 4l and r). This confirms that the residence time selected for the continuous arrangement improved the homogeneity of the mixture, leading to a complete reduction of the silver precursor and to an optimal production of Ag NPs. In this context, the SPR intensity enhancement observed with ageing time when glucose concentration was in defect (r = 5/1), could be attributed to the reduction reaction between free silver ions and extra glucose units from the starch fragmentation [19]. However, when the synthesis was performed under glucose excess conditions (r = 1/1 and r =1/5), the difference between SPR intensity from $t_0$ and $t_2$ was lower because silver ions could be fully reduced in the presence of an excess of reducing agent. Moreover, the starch could improve the stability during the storage periods of 8 and 32 months by keeping a reductant atmosphere, because of its combined effect of stabilizer and co-reducing agent. These results are in agreement with Cheviron et al. [21] who proved the dual influence of starch into the silver nanoparticle suspension, i.e., stabilizer and reducer. They synthesized Ag NPs with and without glucose as reducing agent in presence of starch, and they concluded that Ag NPs size and polydispersity were higher than when glucose was added. They also observed that the SPR peak intensity increased while the reaction time increased, but the intensity of the spectra remained lower than the observed when the reaction mixture contained glucose.

In this vein, it could be suggested that the high starch concentration

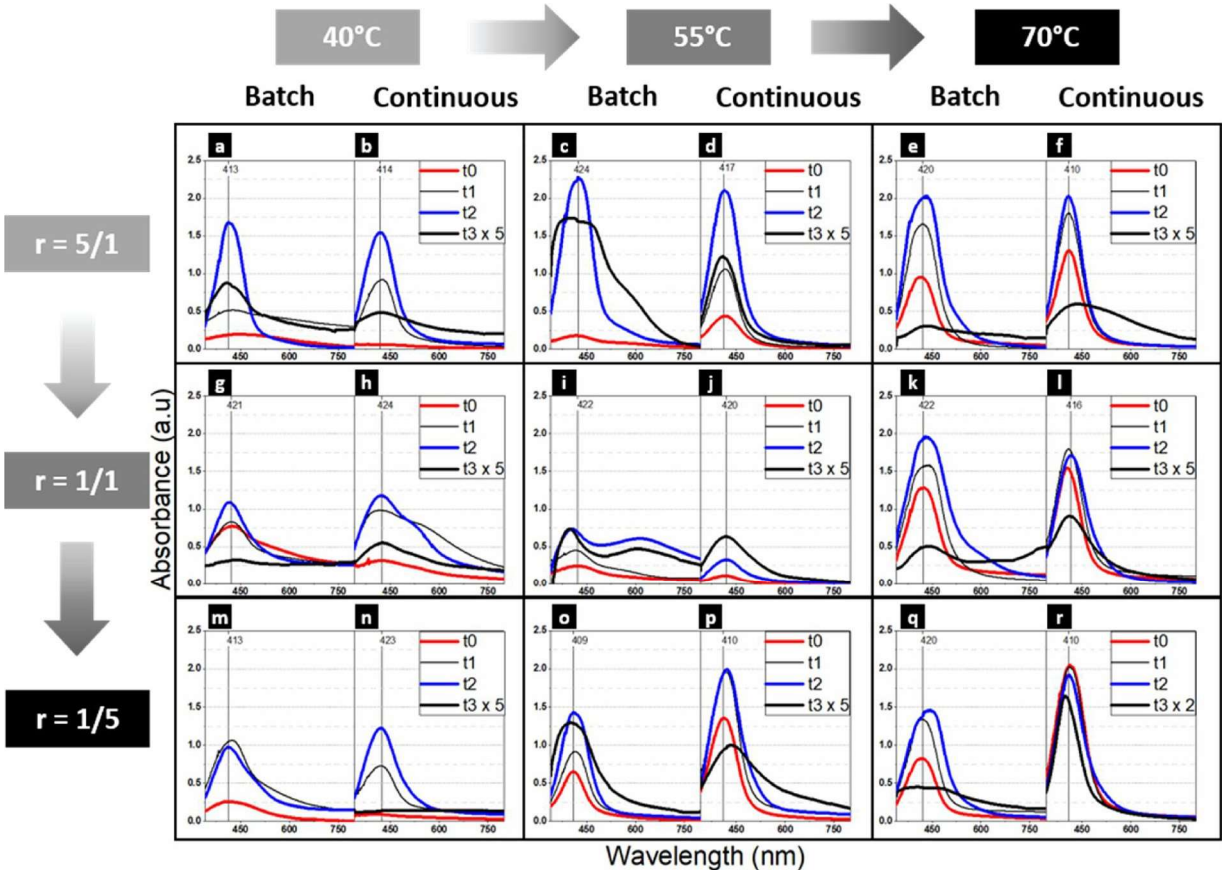


Fig. 4. Evaluation of the colloidal stability of the Ag NPs after different aging periods. UV–vis spectra of the Ag NPs stored at room temperature at $t_0$ (initial synthesis), $t_1$ (after 8 months), $t_2$ (after 32 months) and $t_3$ (after 48 months). Spectra at $t_3$ were enhanced 5 or 2 times ($t_3 \times 5$ or $t_3 \times 2$) for difference highlighting.

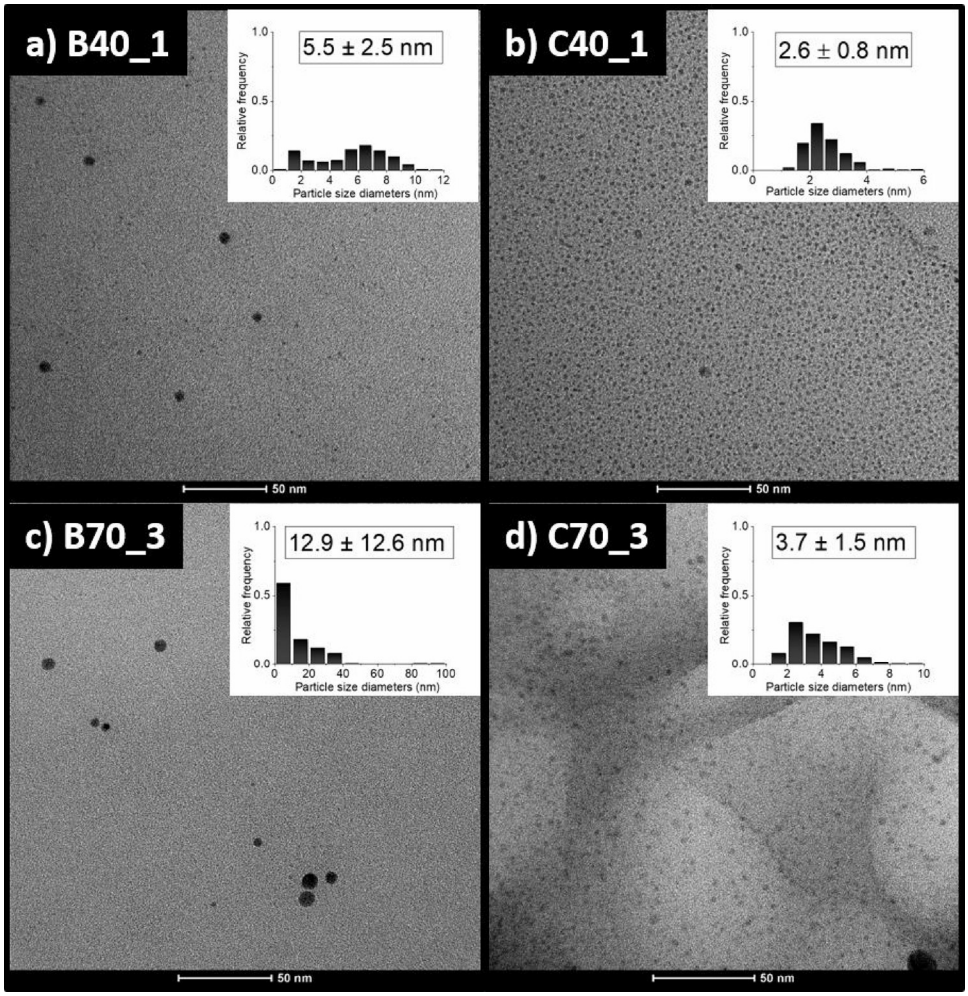


Fig. 5. TEM images and histograms of Ag NPs size distributions of samples prepared at 40 °C with r: 5/1 (top) and 70 °C with r: 1/5 (bottom) after 8 month ($t_1$) storage. See Table 1 for specific name codes.

conducted to a highly stable Ag NPs suspension even for periods above 30 months and that the use of a continuous mixing configuration enables this achievement in a much shorter period of reaction (hours vs. months-years time scale).

TEM analysis of selected Ag NPs samples after 8-months ($t_1$) storage was also performed to evaluate the evolution of the particle size distribution over time (Fig. 5). These measurements were carried out by applying the box plot method (Fig. 6). The horizontal line inside the box represents the median, the top and the bottom of the box represent the upper and lower quartiles, and the vertical length of the box, from upper to lower quartiles, is the interquartile range and therefore 50% of all cases have values within the box. Lines, called whiskers, are drawn from the edge of the box to the maximum and minimum values.

From this analysis, the difference between the size distribution of the Ag NPs synthetized with batch and with the continuous system can be observed. Moreover, Fig. 5 shows TEM images with the mean size and the standard deviation of particles synthetized at 40 °C with r: 5/1 and 70 °C with r: 1/5 by batch and continuous configuration at $t_1$. As it was observed in Fig. 5, the smaller standard deviation of the particle sizes is obtained with the continuous method, leading to particle suspensions with narrower size distributions [24,37].

Finally, the suspensions were studied after being stored for 48 months ($t_3$) under ambient conditions without light protection. UV–vis and TEM results are shown in Figs. 4 and S4, respectively. The UV–vis spectra intensity decreased in all cases. In order to obtain a better comparison, all spectra obtained at $t_3$ were magnified 5 times except for the synthesis condition 70 °C and r = 1/5 in which case the used factor was 2. These results could indicate the dissolution of Ag NPs into the suspension and the agglomeration of the NPs, easily observed by visual inspection of the suspensions. It could be also observed that the width of the spectra from the batch synthesis was much broader than in the analogous experiments performed with the microreactor. It is worth mentioning that the SPR in most of the continuous flow conditions did not change, indicating that the outlasting Ag NPs were still stable in the suspension and kept their size and morphology as it was demonstrated by the TEM images (Fig. S4). However, the particle-size histogram showed a new distribution including larger mean diameters. Although this final distribution at $t_3$, there are still many small NPs with the same diameter measured at $t_1$ (Table 2).

The boxplot graph was also plotted with the Ag NPs size distribution of some suspensions measured after 48 months (Fig. S5). The results are in agreement with the UV–vis spectra presented in Fig. 4. In all the suspensions, larger particles were formed, although there were still nano-sized particles. From the UV–vis results obtained after 48 months, in which the spectra intensity drastically decreased, it could be suggested that during this long term a NPs dissolution process could have occurred.

### 3.3. *Bactericidal assay*

Because of the very small size of the obtained Ag NPs, it was not possible to separate them from the suspension. On the other hand, it is

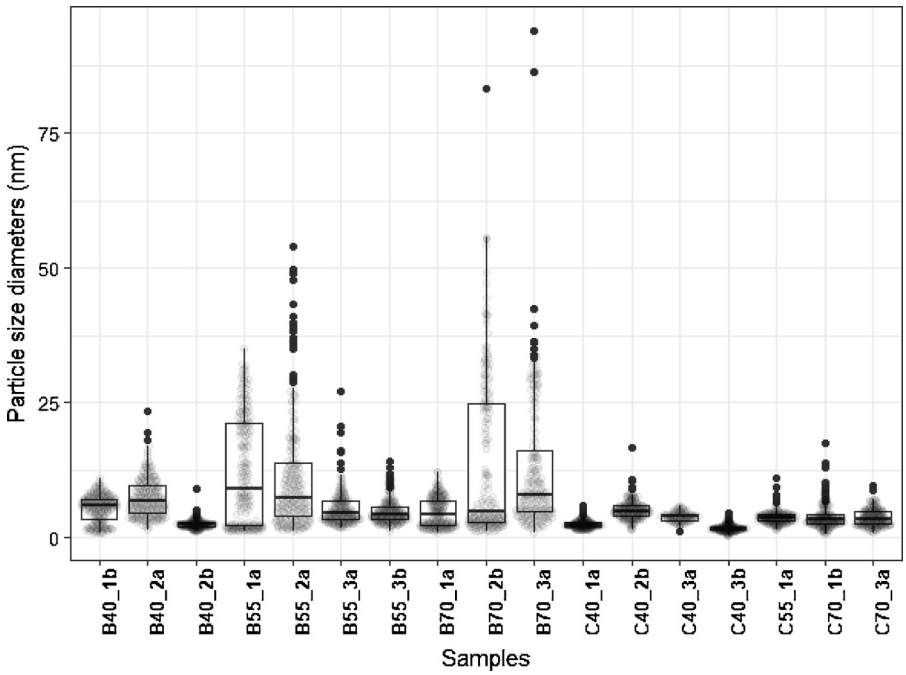


Fig. 6. Boxplot plot distribution of Ag NPs stored for 8 months ($t_1$).

known that the environment of bactericidal source could affect the silver antimicrobial activity. In this context, the obtained Ag NPs bactericidal response was tested without washing the suspension.

The samples synthesized at 70 °C with r = 1/5 (in either batch or continuous conditions) stored for 8 months gave the best optical and morphological response in terms of reproducibility and stability and consequently they were selected to perform bactericidal assays against *E. coli* bacteria. The Ag NPs suspensions were diluted down to 9 and 27 ppm final Ag concentrations. Aqueous solutions of $AgNO_3$ with identical concentrations were used as controls.

Fig. 7 summarizes the effects of the different Ag concentrations of samples and controls on the colony forming units (CFU) of *E. coli* after co-culturing for 20 h. These data fit within the range reported in the literature for the Ag NPs minimal inhibitory concentration (MIC) being around 0.5–50 ppm [38].

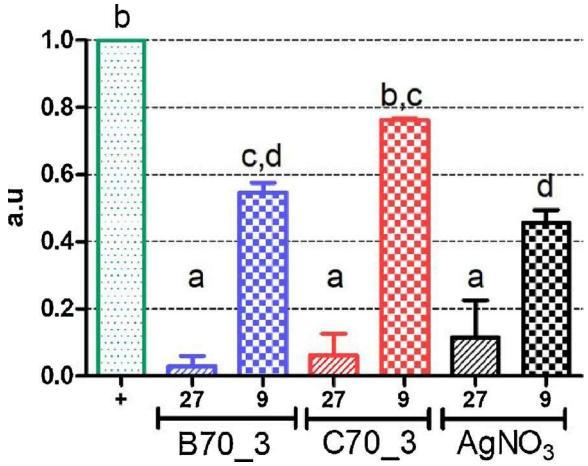


Fig. 7. Bactericidal activity of Ag NPs synthesized by batch (B70_3) and continuous (C70_3) methods and $AgNO_3$ used as control. The concentration of Ag (9 y 27 ppm) is referred to the total amount of silver present in the culture. The concentration of bacteria (CFU/ml) was normalized by the concentration of *E. coli* present in the positive control (+). Each experiment was carried out by triplicate. Different letters indicate significant differences between groups ($p < 0.05$).

According to the statistical analysis, the different letters indicate significant differences between groups. All samples showed significant differences in comparison with the positive control (+, absence of silver species), except for the sample C70_3 that contained 9 ppm of Ag. No significant differences were found among the samples containing 27 ppm of Ag regardless of the type of sample or the preparation method. On the other hand, when the total Ag concentration was 9 ppm, the $AgNO_3$ bactericidal activity was slightly higher compared to the one obtained for Ag NPs.

It has been widely reported that the main bactericidal effect is due to the presence of silver ions [39,40]. Consequently, many factors must be considered to analyze the Ag NPs bactericidal activity. These include all the parameters that promotes the $Ag^+$ release from the particles and their bioavailability, like particle size, oxidation rate, and culture media composition [39–41].

In the first case (27 ppm of Ag concentration), these data suggest that there is a connection between the particle sizes and the bactericidal activity. Despite the fact that C70_3 particles were smaller (mean size 3.74 nm) than B70_3 particles (mean size 12.90 nm), B70_3 presented considerably larger size distribution (standard deviation 12.6 nm) (Fig. 5) and more than 50% of particles were smaller than 10 nm. Therefore, particles from B70_3 and C70_3 could be considered small enough to be completely dissolved as $Ag^+$, showing a similar toxicity than $AgNO_3$. There are strong evidences supporting the higher bactericidal response of smaller Ag NPs due to their high area per volume ratio which generates the presence of a reservoir of Ag ions on the surface of nanoparticles readily available upon dissolution in the culture media [39]. Lalueza et al. [40] claimed that the bactericidal effect depends on the bioavailability of silver ions; the more available, the better biocidal properties of the silver material. In their work, the nanoparticles with average sizes around 100 nm did not show a significant bactericidal effect compared with $AgNO_3$, suggesting a negligible effect on having large and ultra-stable nanoparticles.

In the second case (9 ppm of Ag concentration), it is important to consider that the culture media was not diluted and all the samples and controls were exposed to the same culture media compositions with high content of organic matter (peptone meat extract and yeast extract). Zhang et al. [41] previously studied the dispersion of Ag NPs on

different solvent media and their corresponding bactericidal activity. They observed that $Ag^+$ release is sensitive to the media components. They suggest that the presence of organic material could coat the Ag NPs surface and inhibit the particles dissolution. Consequently, we could propose a hypothesis, that when the lower nanoparticle concentration is used the coating effect of organic matter could be more important retarding the particle dissolution. However further investigations should be performed in order to corroborate this speculation.

Finally, our work agrees with the evidences reported about the influence of the particle size and the media composition on the Ag NPs bactericidal activity. Even more, it was possible to corroborate that the chemicals of the particles synthesis (glucose and starch) do not interfere on the toxicity of the nanoparticles leading to an effective real use of silver ions from the particles by the culture medium.

## 4. Conclusions

This study presents a novel and environmentally benign method for the synthesis of spherical colloidal Ag NPs with excellent characteristics in terms of reproducibility and stability. A green synthesis protocol was followed in which starch and glucose were used as stabilizing agent and reducing agent, respectively. Batch and continuous systems were used in order to compare the reproducibility and the long-term stability of the resulting Ag NPs suspensions. The effects of the reaction temperature and the reagent ratios on the final product characteristic were studied in order to determine the optimal synthesis conditions. From the obtained results, it could be concluded that the optimal silver nanoparticle production was obtained when an Ag/glucose ratio = 1/5 and temperature 70 °C were set, for both batch and continuous systems. However, the continuous system gave the best results in terms of reproducibility and stability in comparison with the batch synthesis under identical reaction conditions but much lower reaction residence times. In fact, a narrower nanoparticle size distribution was obtained with the microreactor compared to the one obtained with the batch reactor. This was because the microfluidic route led to an improved mixing of the reactants, to an elevated conversion, and it enhanced the transfer of mass and heat.

Feeding together both green reagents, glucose and starch, conduced to superior Ag NPs stability, mainly when the synthesis process was performed under continuous regime. The presence of starch was crucial for guaranteeing the Ag NPs stability into the suspension. The main contribution of this work is the analysis of the behavior (optical response, morphology and size distribution) of the Ag NPs suspensions obtained with both arrangements and different reaction conditions after a long-term storage (48 months) without light protection. In all cases, the concentration of Ag NPs decreased after four years because of agglomeration and some dissolution effect. Although for the better synthesis condition observed (70 °C, r = 1/5) the loss of nanoparticle concentration resulted lower than the one observed in the other synthesis conditions.

Finally, it could be concluded that the combination of a green protocol with a continuous production enabled the production of long-term stable Ag NPs with potential bactericidal applications.

## Acknowledgments

The authors from Argentina wish to acknowledge the financial support received from ANPCyT (PICT/11 – 2739), CONICET (PIP/14 - 406) and UNL (CAI+D 50120110100417LI). Thanks are also given to Prof. Guillermina Amrein for the English language editing and to the students Santiago Ibarlín, Diamela Grosso and Francisco Wisniewski for their technical assistance with the laboratory tasks. Esteban Gioria also wants to thank to the Santa Fe Bank Foundation for the partial financing of this work within the student grant "Technological Innovation 2014".

Financial support from MINECO (Spain) with project PRI-PIBAR-2011-1366 and the CIBER-BBN is gratefully acknowledged. CIBER-BBN is an initiative funded by the VI National R&D&i Plan 2008–2011, Iniciativa Ingenio 2010, Consolider Program, CIBER Actions and financed by the Instituto de Salud Carlos III (Spain) with assistance from the European Regional Development Fund. The synthesis of materials has been performed by the Platform of Production of Biomaterials and Nanoparticles of the NANOBIOSIS ICTS, more specifically by the Nanoparticle Synthesis Unit of the CIBER in Bioengineering, Biomaterials & Nanomedicine (CIBER-BBN). The TEM studies were conducted at the Laboratorio de Microscopias Avanzadas, Instituto de Nanociencia de Aragón, Universidad de Zaragoza, Spain.

## Appendix A. Supplementary data

Supplementary material related to this article can be found, in the online version, at doi:https://doi.org/10.1016/j.jece.2018.07.039.

## References

[1] A. Regiel-Futyra, M. Kus-Liśkiewicz, V. Sebastian, S. Irusta, M. Arruebo, G. Stochel, A. Kyzioł, Development of noncytotoxic chitosan–gold nanocomposites as efficient antibacterial materials, ACS Appl. Mater. Interfaces 7 (2015) 1087.
[2] G. Mendoza, A. Regiel-Futyra, V. Andreu, V. Sebastián, A. Kyzioł, G. Stochel, M. Arruebo, Bactericidal effect of gold–chitosan nanocomposites in coculture models of pathogenic bacteria and human macrophages, ACS Appl. Mater. Interfaces 9 (2017) 17693.
[3] Y.N. Slavin, J. Asnis, U.O. Häfeli, H. Bach, Metal nanoparticles: understanding the mechanisms behind antibacterial activity, J. Nanobiotechnol. 15 (2017) 65.
[4] L. Wang, C. Hu, L. Shao, The antimicrobial activity of nanoparticles: present situation and prospects for the future, Int. J. Nanomed. 12 (2017) 1227.
[5] P.V. AshaRani, G. Low Kah Mun, M.P. Hande, S. Valiyaveettil, Cytotoxicity and genotoxicity of silver nanoparticles in human cells, ACS Nano 3 (2009) 279.
[6] S. Arora, J.M. Rajwade, K.M. Paknikar, Nanotoxicology and in vitro studies: the need of the hour, Toxicol. Appl. Pharmacol. 258 (2012) 151.
[7] A. Kumar, P.K. Vemula, P.M. Ajayan, G. John, Silver-nanoparticle-embedded antimicrobial paints based on vegetable oil, Nat. Mater. 7 (2008) 236.
[8] P. Ilana, A. Guy, P. Nina, G. Geoffrey, M. Serguei, G. Aharon, Sonochemical coating of silver nanoparticles on textile fabrics (nylon, polyester and cotton) and their antibacterial activity, Nanotechnology 19 (2008) 245705.
[9] T. Quang Huy, N. Van Quy, L. Anh-Tuan, Silver nanoparticles: synthesis, properties, toxicology, applications and perspectives, Adv. Nat. Sci.: Nanosci. Nanotechol. 4 (2013) 033001.
[10] P.T. Anastas, T.C. Williamson, Green chemistry: an overview, in: ACS (Ed.), Green Chem. American Chemical Society, Washington, DC, 1996, pp. 1–17.
[11] K.B. Narayanan, N. Sakthivel, Biological synthesis of metal nanoparticles by microbes, Adv. Colloid Interface Sci. 156 (2010) 1.
[12] S. Shamaila, A.K.L. Sajjad, N.-u.-A. Ryma, S.A. Farooqi, N. Jabeen, S. Majeed, I. Farooq, Advancements in nanoparticle fabrication by hazard free eco-friendly green routes, Appl. Mater. Today 5 (2016) 150.
[13] H. Duan, D. Wang, Y. Li, Green chemistry for nanoparticle synthesis, Chem. Soc. Rev. 44 (2015) 5778.
[14] M.M. Kemp, A. Kumar, D. Clement, P. Ajayan, S. Mousa, R.J. Linhardt, Hyaluronan- and heparin-reduced silver nanoparticles with antimicrobial properties, Nanomedicine 4 (2009) 421.
[15] E. Filippo, D. Manno, A. Buccolieri, M. Di Giulio, A. Serra, Shape-dependent plasmon resonances of Ag nanostructures, Superlattices Microstruct. 47 (2010) 66.
[16] M.H. El-Rafie, H.B. Ahmed, M.K. Zahran, Facile precursor for synthesis of silver nanoparticles using alkali treated maize starch, Int. Sch. Res. Notices 2014 (2014) 12.
[17] N. Vigneshwaran, R.P. Nachane, R.H. Balasubramanya, P.V. Varadarajan, A novel one-pot' green' synthesis of stable silver nanoparticles using soluble starch, Carbohydr. Res. 341 (2006) 2012.
[18] P. Raveendran, J. Fu, S.L. Wallen, Completely "Green" synthesis and stabilization of metal nanoparticles, J. Am. Chem.Soc. 125 (2003) 13940.
[19] M. Singh, I. Sinha, R.K. Mandal, Role of pH in the green synthesis of silver nanoparticles, Mater. Lett. 63 (2009) 425.
[20] S. Chairam, C. Poolperm, E. Somsook, Starch vermicelli template-assisted synthesis of size/shape-controlled nanoparticles, Carbohydr. Polym. 75 (2009) 694.
[21] P. Cheviron, F. Gouanvé, E. Espuche, Green synthesis of colloid silver nanoparticles and resulting biodegradable starch/silver nanocomposites, Carbohydr. Polym. 108 (2014) 291.
[22] V. Sebastian, M. Arruebo, J. Santamaria, Reaction engineering strategies for the production of inorganic nanomaterials, Small 10 (2014) 835.
[23] J.B. Edel, R. Fortt, J.C. deMello, A.J. deMello, Microfluidic routes to the controlled production of nanoparticles, Chem. Commun. 10 (2002) 1136.
[24] L. Gutierrez, L. Gomez, S. Irusta, M. Arruebo, J. Santamaria, Comparative study of the synthesis of silica nanoparticles in micromixer–microreactor and batch reactor systems, Chem. Eng. J. 171 (2011) 674.
[25] D.K. Božanić, S. Dimitrijević-Branković, N. Bibić, A.S. Luyt, V. Djoković, Silver

nanoparticles encapsulated in glycogen biopolymer: morphology, optical and antimicrobial properties, Carbohydr. Polym. 83 (2011) 883.
[26] M. Darroudi, M.B. Ahmad, R. Zamiri, A.K. Zak, A.H. Abdullah, N.A. Ibrahim, Time-dependent effect in green synthesis of silver nanoparticles, Int. J. Nanomed. 6 (2011) 677.
[27] Z. Shervani, Y. Yamamoto, Carbohydrate-directed synthesis of silver and gold nanoparticles: effect of the structure of carbohydrates and reducing agents on the size and morphology of the composites, Carbohydr. Res. 346 (2011) 651.
[28] S.M. Ghaseminezhad, S. Hamedi, S.A. Shojaosadati, Green synthesis of silver nanoparticles by a novel method: comparative study of their properties, Carbohydr. Polym. 89 (2012) 467.
[29] S. Horikoshi, T. Sumi, N. Serpone, A hybrid microreactor/microwave high-pressure flow system of a novel concept design and its application to the synthesis of silver nanoparticles, Chem. Eng. Process. Process Intensif. 73 (2013) 59.
[30] ImageJ, https://imagej.nih.gov/ij/index.html, 1997 (Accessed 6 April 2018).
[31] R, https://www.r-project.org/, 1993 (Accessed 6 April 2018).
[32] X.C. Jiang, W.M. Chen, C.Y. Chen, S.X. Xiong, A.B. Yu, Role of temperature in the growth of silver nanoparticles through a synergetic reduction approach, Nanoscale Res. Lett. 6 (2011) 32.
[33] C.C. Bonatto, L.P. Silva, Higher temperatures speed up the growth and control the size and optoelectrical properties of silver nanoparticles greenly synthesized by cashew nutshells, Ind. Crops Prod. 58 (2014) 46.
[34] L. Gomez, M. Arruebo, V. Sebastian, L. Gutierrez, J. Santamaria, Facile synthesis of $SiO_2$-Au nanoshells in a three-stage microfluidic system, J. Mater. Chem. 22 (2012) 21420.
[35] S.K. Batabyal, C. Basu, A.R. Das, G.S. Sanyal, Green chemical synthesis of silver nanowires and microfibers using starch, J. Biobased Mater. Bioenergy 1 (2007) 143.
[36] I. Ortiz de Solorzano, L. Uson, A. Larrea, M. Miana, V. Sebastian, M. Arruebo, Continuous synthesis of drug-loaded nanoparticles using microchannel emulsification and numerical modeling: effect of passive mixing, Int. J. Nanomed. 11 (2016) 3397.
[37] G.A. Patil, M.L. Bari, B.A. Bhanvase, V. Ganvir, S. Mishra, S.H. Sonawane, Continuous synthesis of functional silver nanoparticles using microreactor: Effect of surfactant and process parameters, Chem. Eng. Process. Process Intensif. 62 (2012) 69.
[38] N.R. Chowdhury, M. MacGregor-Ramiasa, P. Zilm, P. Majewski, K. Vasilev, 'Chocolate' silver nanoparticles: synthesis, antibacterial activity and cytotoxicity, J. Colloid Interface Sci. 482 (2016) 151.
[39] L. Kvítek, A. Panáček, J. Soukupová, M. Kolář, R. Večeřová, R. Prucek, M. Holecová, R. Zbořil, Effect of surfactants and polymers on stability and antibacterial activity of silver nanoparticles (NPs), J. Phys. Chem. C 112 (2008) 5825.
[40] P. Lalueza, M. Monzón, M. Arruebo, J. Santamaría, Bactericidal effects of different silver-containing materials, Mater. Res. Bull. 46 (2011) 2070.
[41] H. Zhang, J.A. Smith, V. Oyanedel-Craver, The effect of natural water conditions on the anti-bacterial performance and stability of silver nanoparticles capped with different polymers, Water Res. 46 (2012) 691.

# Supplementary material

# Natural Polysaccharides and microfluidics: a win-win combination towards the green and continuous production of long-term stable silver nanoparticles

*Antonella Giorello [a], Esteban Gioria [a], Jose L. Hueso [b, c], Victor Sebastian [b, c], Manuel Arruebo [b, c], Carolina Veaute [d], Laura Gutierrez [a,*]*

[a] Instituto de Investigaciones en Catálisis y Petroquímica, INCAPE, (FIQ, UNL-CONICET), Santiago del Estero 2829, S3000 Santa Fe, Argentina

[b] Institute of Nanoscience of Aragon (INA) and Department of Chemical and Environmental Engineering, Edificio I+D+i, Campus Rio Ebro, 50018, Zaragoza, Spain.

[c] Networking Research Center on Bioengineering, Biomaterials and Nanomedicine (CIBER-BBN), 28029, Madrid, Spain.

[d] Laboratorio de Inmunología Básica, FBCB, Universidad Nacional del Litoral, UNL. Ciudad Universitaria UNL, Ruta Nacional Nº 168, km 472. S3000ZAA. Santa Fe. Argentina.

*E-mail: lgutier@fiq.unl.edu.ar

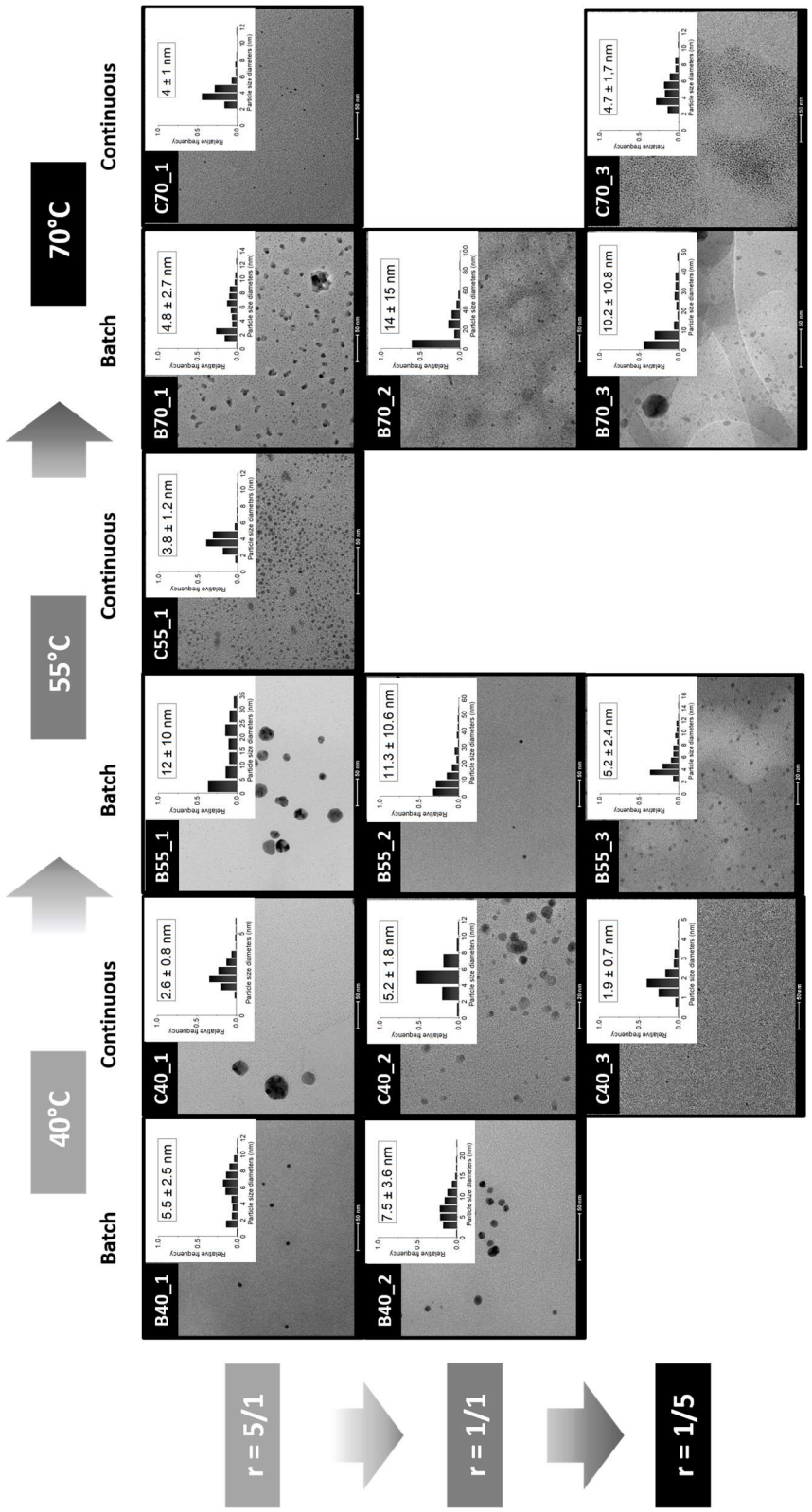


**Figure S1.** TEM images and particle size distribution of some representative Ag NPs suspension at t0.

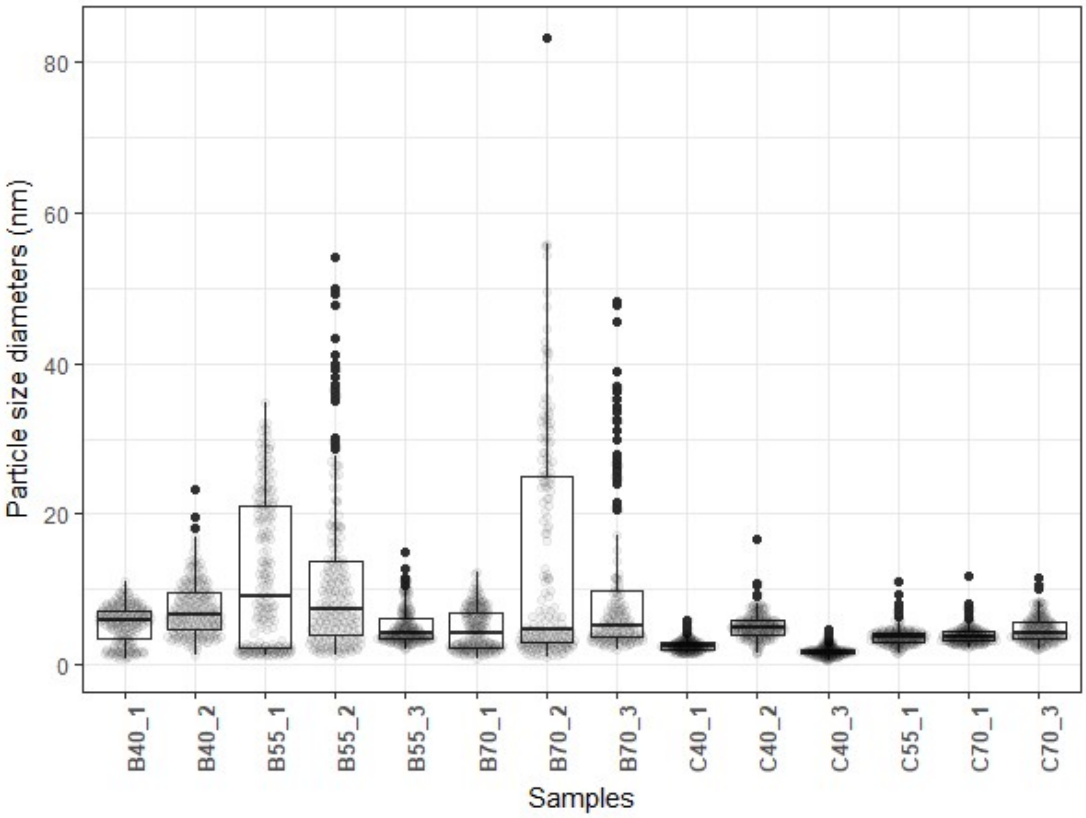


**Figure S2.** Box plot of size particles distribution of Ag NPs at t0.

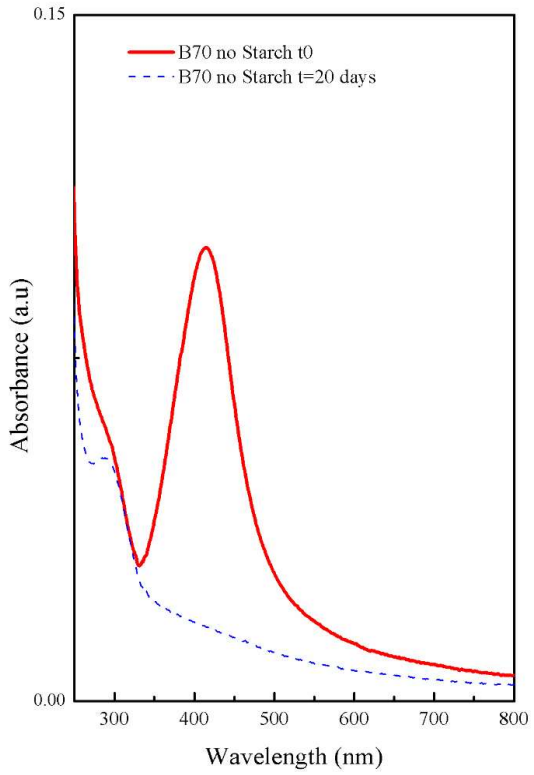


**Figure S3.** Effect of the absence of starch on the silver reducibility and on the AgNPs stability.

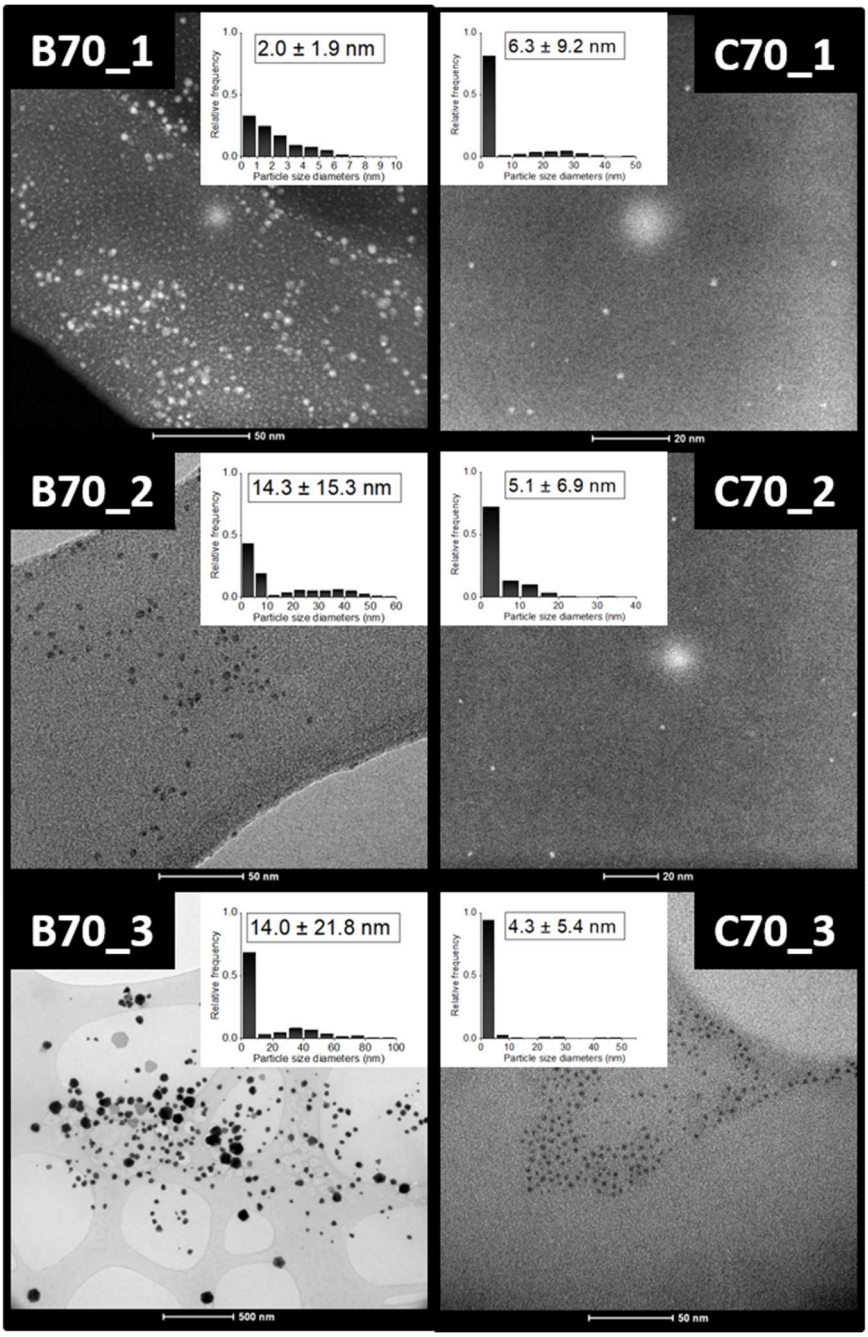


**Figure S4.** TEM analysis of selected Ag NPs samples after 48-months ($t_2$) storage.

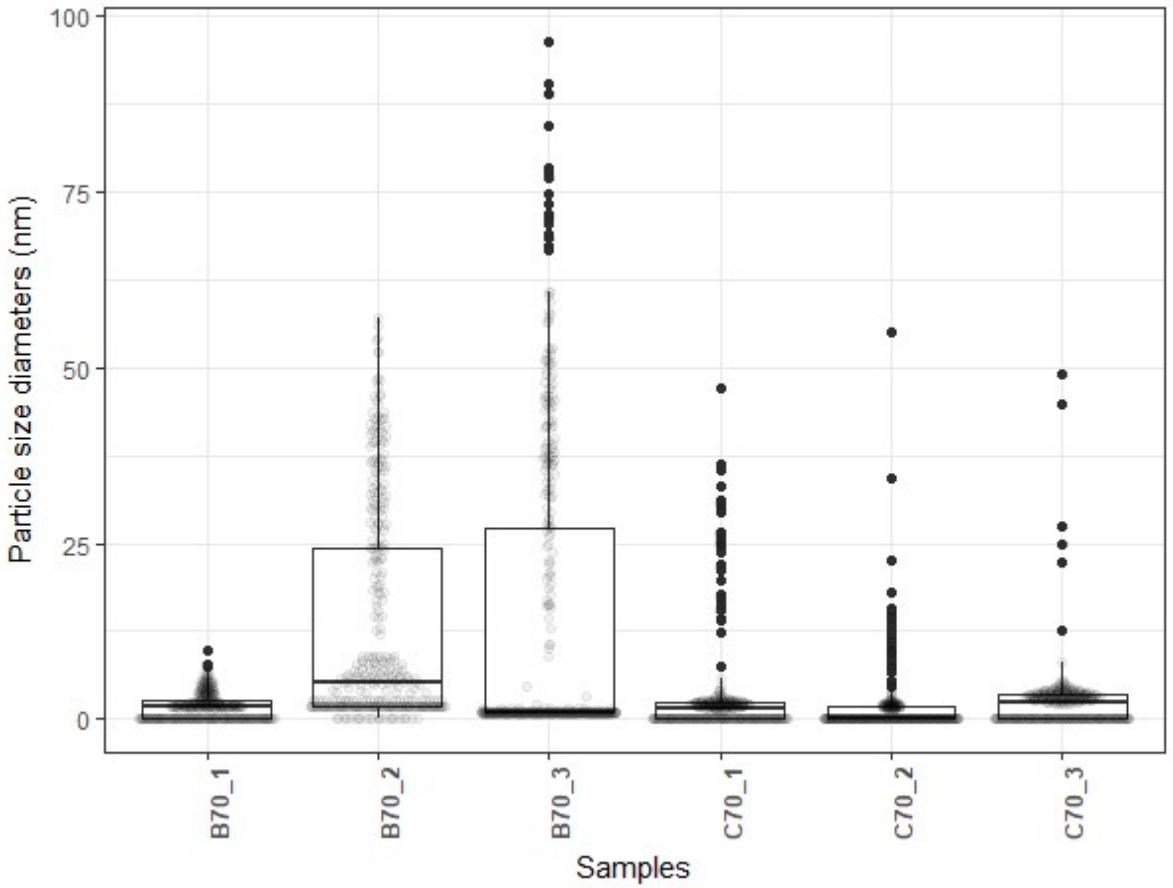


**Figure S5.** Box plot of size particles distribution of Ag NPs stored 48 months.

**Table S1.** Ag NPs synthesis method (batch or continuous) and the type of reducer agent (with green or toxic environmental effects) evaluated in literature in the last ten years.

| Synthesis method | Reducer Agent | | Reference |
|---|---|---|---|
| | Green | Toxic | |
| Batch | Ascorbic acid | | [1, 2] |
| Batch | Cocoa extract | | [3] |
| Batch | Citrate | | [4] |
| Batch | Glucose | | [5-11] |
| Batch | Hydroquinone | | [12] |
| Batch | Lactose | | [13] |
| Batch | Microorganism | | [14] |
| Batch | Plant extract | | [15, 16] |
| Batch | PVP | | [17] |
| Batch | Tanic acid | | [18] |
| Batch | Tochoferol | | [19] |
| Batch | | NaH | [20] |
| Batch | | $NaBH_4$ | [21-24] |
| Batch | | $N_2H_4$ | [25] |
| Batch | | $NaBH_4$ / $N_2H_4$ | [26] |
| Continuous | Cinnamomum camphora extract | | [27] |
| Continuous | Cacumen Platycladi extract | | [28] |
| Continuous | Glucose | | [29] |
| Continuous | Oleic Acid | | [30] |
| Continuous | Tanic acid | | [31] |
| Continuous | | $NaBH_4$ | [32-34] |

[1] K. Chamakura, R. Perez-Ballestero, Z. Luo, S. Bashir, J. Liu, Comparison of bactericidal activities of silver nanoparticles with common chemical disinfectants, Colloids Surf. B Biointerfaces, 84 (2011) p. 88.

[2] Z. Khan, T. Singh, J.I. Hussain, A.Y. Obaid, S.A. Al-Thabaiti, E.H. El-Mossalamy, Starch-directed green synthesis, characterization and morphology of silver nanoparticles, Colloids Surf. B Biointerfaces, 102 (2013) p. 578.

[3] N.R. Chowdhury, M. MacGregor-Ramiasa, P. Zilm, P. Majewski, K. Vasilev, 'Chocolate' silver nanoparticles: Synthesis, antibacterial activity and cytotoxicity, J. Colloid Interface Sci., 482 (2016) p. 151.
[4] A.M. Pandian, C. Karthikeyan, M. Rajasimman, M.G. Dinesh, Synthesis of silver nanoparticle and its application, Ecotoxicol. Environ. Saf., 121 (2015) p. 211.
[5] P. Raveendran, J. Fu, S.L. Wallen, Completely "Green" Synthesis and Stabilization of Metal Nanoparticles, J. Am. Chem. Soc., 125 (2003) p. 13940.
[6] M. Singh, I. Sinha, R.K. Mandal, Role of pH in the green synthesis of silver nanoparticles, Mater. Lett., 63 (2009) p. 425.
[7] D.K. Božanić, S. Dimitrijević-Branković, N. Bibić, A.S. Luyt, V. Djoković, Silver nanoparticles encapsulated in glycogen biopolymer: Morphology, optical and antimicrobial properties, Carbohydr. Polym., 83 (2011) p. 883.
[8] M. Darroudi, M.B. Ahmad, R. Zamiri, A.K. Zak, A.H. Abdullah, N.A. Ibrahim, Time-dependent effect in green synthesis of silver nanoparticles, Int. J. Nanomed., 6 (2011) p. 677.
[9] Z. Shervani, Y. Yamamoto, Carbohydrate-directed synthesis of silver and gold nanoparticles: effect of the structure of carbohydrates and reducing agents on the size and morphology of the composites, Carbohydr. Res., 346 (2011) p. 651.
[10] S.M. Ghaseminezhad, S. Hamedi, S.A. Shojaosadati, Green synthesis of silver nanoparticles by a novel method: comparative study of their properties, Carbohydr. Polym., 89 (2012) p. 467.
[11] P. Cheviron, F. Gouanvé, E. Espuche, Green synthesis of colloid silver nanoparticles and resulting biodegradable starch/silver nanocomposites, Carbohydr. Polym., 108 (2014) p. 291.
[12] Q. Bao, D. Zhang, P. Qi, Synthesis and characterization of silver nanoparticle and graphene oxide nanosheet composites as a bactericidal agent for water disinfection, J. Colloid Interface Sci., 360 (2011) p. 463.
[13] X. Zhang, H. Niu, J. Yan, Y. Cai, Immobilizing silver nanoparticles onto the surface of magnetic silica composite to prepare magnetic disinfectant with enhanced stability and antibacterial activity, Colloids Surf. A Physicochem. Eng. As., 375 (2011) p. 186.
[14] B. Buszewski, K. Rafińska, P. Pomastowski, J. Walczak, A. Rogowska, Novel aspects of silver nanoparticles functionalization, Colloids Surf. A Physicochem. Eng. As., 506 (2016) p. 170.
[15] M. Gulsonbi, S. Parthasarathy, K. Bharat Raj, V. Jaisankar, Green synthesis, characterization and drug delivery applications of a novel silver/carboxymethylcellulose – poly(acrylamide) hydrogel nanocomposite, Ecotoxicol. Environ. Saf., 134 (2016) p. 421.
[16] D. Rithesh Raj, S. Prasanth, T.V. Vineeshkumar, C. Sudarsanakumar, Surface plasmon resonance based fiber optic dopamine sensor using green synthesized silver nanoparticles, Sensors Actuators B: Chem., 224 (2016) p. 600.
[17] L. Chen, L. Zheng, Y. Lv, H. Liu, G. Wang, N. Ren, D. Liu, J. Wang, R.I. Boughton, Chemical assembly of silver nanoparticles on stainless steel for antimicrobial applications, Surf. Coat. Technol., 204 (2010) p. 3871.
[18] I. Medina-Ramirez, S. Bashir, Z. Luo, J.L. Liu, Green synthesis and characterization of polymer-stabilized silver nanoparticles, Colloids Surf. B Biointerfaces, 73 (2009) p. 185.
[19] S. Shankar, J.-W. Rhim, Tocopherol-mediated synthesis of silver nanoparticles and preparation of antimicrobial PBAT/silver nanoparticles composite films, LWT Food Sci. Technol., 72 (2016) p. 149.
[20] L. Balan, J.-P. Malval, R. Schneider, D. Burget, Silver nanoparticles: New synthesis, characterization and photophysical properties, Mater. Chem. Phys., 104 (2007) p. 417.
[21] O. Choi, K.K. Deng, N.J. Kim, L. Ross, Jr., R.Y. Surampalli, Z. Hu, The inhibitory effects of silver nanoparticles, silver ions, and silver chloride colloids on microbial growth, Water Res., 42 (2008) p. 3066.

[22] P.V. AshaRani, G. Low Kah Mun, M.P. Hande, S. Valiyaveettil, Cytotoxicity and Genotoxicity of Silver Nanoparticles in Human Cells, ACS Nano, 3 (2009) p. 279.
[23] H.J. Lee, S.G. Lee, E.J. Oh, H.Y. Chung, S.I. Han, E.J. Kim, S.Y. Seo, H.D. Ghim, J.H. Yeum, J.H. Choi, Antimicrobial polyethyleneimine-silver nanoparticles in a stable colloidal dispersion, Colloids Surf. B Biointerfaces, 88 (2011) p. 505.
[24] B. Sadeghi, F.S. Garmaroudi, M. Hashemi, H.R. Nezhad, A. Nasrollahi, S. Ardalan, S. Ardalan, Comparison of the anti-bacterial activity on the nanosilver shapes: Nanoparticles, nanorods and nanoplates, Adv. Powder Technol., 23 (2012) p. 22.
[25] M. Guzman, J. Dille, S. Godet, Synthesis and antibacterial activity of silver nanoparticles against gram-positive and gram-negative bacteria, Nanomedicine, 8 (2012) p. 37.
[26] X. Zhao, B. Chen, C. Li, T. Wang, J. Zhang, X. Jiao, D. Chen, Large-scale synthesis of size-controllable silver nanoplates and their application in detecting strong oxidants in aqueous solutions, Chem. Eng. J., 285 (2016) p. 690.
[27] J. Huang, L. Lin, Q. Li, D. Sun, Y. Wang, Y. Lu, N. He, K. Yang, X. Yang, H. Wang, W. Wang, W. Lin, Continuous-Flow Biosynthesis of Silver Nanoparticles by Lixivium of Sundried Cinnamomum camphora Leaf in Tubular Microreactors, Ind. Eng. Chem. Res., 47 (2008) p. 6081.
[28] H. Liu, J. Huang, D. Sun, L. Lin, W. Lin, J. Li, X. Jiang, W. Wu, Q. Li, Microfluidic biosynthesis of silver nanoparticles: Effect of process parameters on size distribution, Chem. Eng. J., 209 (2012) p. 568.
[29] S. Horikoshi, T. Sumi, N. Serpone, A hybrid microreactor/microwave high-pressure flow system of a novel concept design and its application to the synthesis of silver nanoparticles, Chem. Eng. Process. Process Intensif., 73 (2013) p. 59.
[30] D.V.R. Kumar, M. Kasture, A.A. Prabhune, C.V. Ramana, B.L.V. Prasad, A.A. Kulkarni, Continuous flow synthesis of functionalized silver nanoparticles using bifunctional biosurfactants, Green Chem., 12 (2010) p. 609.
[31] S.K. Sivaraman, I. Elango, S. Kumar, V. Santhanam, A green protocol for room temperature synthesis of silver nanoparticles in seconds, Curr. Sci., 97 (2009) p. 1055.
[32] A. Knauer, A. Csáki, F. Möller, C. Hühn, W. Fritzsche, J.M. Köhler, Microsegmented Flow-Through Synthesis of Silver Nanoprisms with Exact Tunable Optical Properties, J. Phys. Chem. C, 116 (2012) p. 9251.
[33] G.A. Patil, M.L. Bari, B.A. Bhanvase, V. Ganvir, S. Mishra, S.H. Sonawane, Continuous synthesis of functional silver nanoparticles using microreactor: Effect of surfactant and process parameters, Chem. Eng. Process. Process Intensif., 62 (2012) p. 69.
[34] L. Xu, J. Peng, M. Yan, D. Zhang, A.Q. Shen, Droplet synthesis of silver nanoparticles by a microfluidic device, Chem. Eng. Process. Process Intensif., 102 (2016) p. 186.